A Joint Distribution System State Estimation Framework via Deep Actor-Critic Learning Method

Yuxuan Yuan, *Graduate Student Member, IEEE*, Kaveh Dehghanpour, Zhaoyu Wang, *Senior Member, IEEE*, and Fankun Bu, *Graduate Student Member, IEEE*

***Abstract*—Due to the increasing penetration of volatile distributed photovoltaic (PV) resources, real-time monitoring of customers at the grid-edge has become a critical task. However, this requires solving the distribution system state estimation (DSSE) jointly for both primary and secondary levels of distribution grids, which is computationally complex and lacks scalability to large-scale systems. To achieve real-time solutions for DSSE, we present a novel hierarchical reinforcement learning-aided framework: at the first layer, a weighted least squares (WLS) algorithm solves the DSSE over primary medium-voltage feeders; at the second layer, deep actor-critic (A-C) modules are trained for each secondary transformer using measurement residuals to estimate the states of low-voltage circuits and capture the impact of PVs at the grid-edge. While the A-C parameter learning process takes place offline, the trained A-C modules are deployed online for fast secondary grid state estimation; this is the key factor in the scalability and computational efficiency of the framework. To maintain monitoring accuracy, the two levels exchange boundary information with each other at the secondary nodes, including transformer voltages (first layer to second layer) and active/reactive total power injection (second layer to first layer). This interactive information passing strategy results in a closed-loop structure that is able to track optimal solutions at both layers in a few iterations. We have performed numerical experiments using real utility data and feeder models to verify the performance of the proposed framework.**

***Index Terms*—Actor-critic method, joint distribution system state estimation, distributed PV generation, secondary distribution network.**

Nomenclature

A-C	Actor-critic
BCSE	Branch current state estimation
DSSE	Distribution system state estimation
DNN	Deep neural network
KDE	Kernel density estimation
LV	Low voltage
MV	Medium voltage
PV	Photovoltaic
PDF	Probability density function
SM	Smart meter
TDE	Temporal difference error
$\boldsymbol{c}_n$	External input vector for secondary transformer n
G	Gain matrix
H	Jacobian matrix
$I_{Re,n}, I_{Im,n}$	Real and imaginary current components of secondary transformer n.
J	Sum of squared residuals
l_c	Learning rate of A-C module
N_{MV}	Number of nodes in MV system
N_{LV}	Number of nodes in LV system
$\hat{\boldsymbol{p}}_{\boldsymbol{s}}$	Active power injections of secondary transformers
$\hat{\boldsymbol{q}}_{\boldsymbol{s}}$	Reactive power injections of secondary transformers
$\hat{r}_n$	Approximate measurement residuals of secondary transformer n
r_n	Actual measurement residuals of secondary transformer n
$\boldsymbol{u}_n$	Exploratory perturbation for secondary transformer n
V_n	Estimated voltage of secondary transformer n
W	Weight matrix
W_{MW}	Weight matrix of MV network sensors
W_{p_s}, W_{q_s}	Weight matrices of secondary network states
$\boldsymbol{x}_{\boldsymbol{p}}$	Vector of primary network states
$\boldsymbol{x}_{\boldsymbol{s},\boldsymbol{n}}$	Real and imaginary current components of secondary network n
$\boldsymbol{z}_{\boldsymbol{s},\boldsymbol{n}}$	SM voltage and energy measurements of secondary network n
$\boldsymbol{z}_{\boldsymbol{MV}}$	MV network sensor measurements
$\mathcal{A}_\mu, \mathcal{A}_\Sigma$	DNNs for parameterizing μ_n and Σ_n
$\boldsymbol{\alpha}_n$	Parameters of critic for secondary transformer n
δ	Threshold for BCSE
π_n	Policy function of actor for secondary transformer n

Manuscript received September 24, 2021; revised January 21, 2022; accepted February 26, 2022. This work was supported in part by the National Science Foundation under Grant EPCN 2042314, and in part by Advanced Grid Modeling Program at the U.S. Department of Energy Office of Electricity under Grant DE-OE0000875. Paper no. TPWRS-01520-2021. *(Corresponding author: Zhaoyu Wang.)*

The authors are with the Department of Electrical and Computer Engineering, Iowa State University, Ames, IA 50011 USA (e-mail: yuanyx@iastate.edu; kavehdeh1@gmail.com; wzy@iastate.edu; fbu@iastate.edu).

Color versions of one or more figures in this article are available at https://doi.org/10.1109/TPWRS.2022.3155649.

Digital Object Identifier 10.1109/TPWRS.2022.3155649

μ_n	Mean vector of secondary transformer n states
$\boldsymbol{\theta_n}, \boldsymbol{\gamma_n}$	Learning parameters of DNNs in actor
Σ_n	Covariance matrix of secondary transformer n states
$\Sigma_{I_{Re,n}}, \Sigma_{I_{Im,n}}$	Components of Σ_n corresponding to the states $I_{Re,n}$ and $I_{Im,n}$
$\sigma^2_{p_{s,n}}, \sigma^2_{q_{s,n}}$	Variances of net active and reactive power for secondary transformer n
$\nabla_{\boldsymbol{\alpha_n}} \mathcal{C}$	Gradient of the critic DNN
$\nabla_{\boldsymbol{\theta_n}} \pi_n$	Gradient of policy function with respect to $\boldsymbol{\theta_n}$
$\nabla_{\boldsymbol{\gamma_n}} \pi_n$	Gradient of policy function with respect to $\boldsymbol{\gamma_n}$

I. Introduction

As MORE stochastic customer-owned distributed resources, such as photovoltaic (PV) power generators, are connected to low voltage (LV) secondary distribution grids, an urgent need grows for accurate and efficient system monitoring [1]. Specifically, topological details of secondary networks and the real-time measurements of customers have to be incorporated into distribution system state estimation (DSSE) to accurately capture voltage fluctuations across LV systems and quantify the impacts of these variations on medium voltage (MV) primary distribution feeders. Recent years have seen a rapid growth in the deployment of smart meters (SMs), providing a good opportunity to achieve this [2].

A. Literature Review and Challenges

Most existing works have provided distribution system state estimation (DSSE) solutions only in a *disjoint manner* (i.e., by decoupling primary and secondary networks); these works can be roughly categorized into two general groups: *(1) Primary Grid DSSE:* multiple DSSE methods have been provided for MV primary distribution feeders, while aggregating all LV resources at the secondary transformers and disregarding the secondary grid topology and parameters [3]–[11]. The basic approach is to compensate for lack of a detailed secondary model in DSSE by estimating LV network losses, which can then be used as pseudo-measurements to revise measurement aggregation [12]. *(2) Secondary Grid DSSE:* Another group of papers has explored DSSE techniques for LV secondary networks while simplifying primary MV feeders [13]–[19]. Here, the primary feeder has been generally modeled as a constant voltage source to which the secondary network is connected.

All these papers use the SM measurements to monitor only one level of the distribution network and do not permit comprehensive monitoring of the distribution network at the LV and MV levels. Some previous works can be extended to a unified model of all primary and secondary circuits. However, such extensions can lead to computational blow-up due to the extremely large size of joint primary-secondary systems, especially for urban systems. In other words, these methods can take a time delay of several minutes in real-time applications, which may not truly reflect the current system states [20]. This lack of scalability contributes to unacceptable time delays in obtaining system states and hinders the online monitoring of modern distribution grids. Also, due to their disjoint approaches towards system monitoring, previous works in both groups can fail to accurately capture the potential mutual impacts of LV and MV networks on each other; furthermore, the mutual impacts of several neighboring secondary networks connected to the same primary feeder have not been quantified. Consequently, disjoint DSSE solvers become untenable and less accurate as conventional distribution systems move towards more active grids with higher penetration of renewable resources that can cause multi-directional power flow across the grid and poses a great challenge for high-confidence pseudo-measurement generation. Under this new situation, previous modeling assumptions, such as constant voltage levels in primary feeders, can become too strong. The impact of secondary network topology on voltage fluctuations at the grid-edge can no longer be ignored.

To meet these problems, a natural solution is to devise a DSSE solution that is able to jointly monitor primary and secondary networks, referred to as joint DSSE. As per our knowledge on the topic, studies of joint DSSE are still limited. Few recent papers [21], [22] have proposed distributed multi-level architectures for performing DSSE at LV and MV levels. However, in these cases, several critical questions remain open, which may challenge the practical deployment of these joint DSSE methods. 1) The DSSE algorithms only have an open-loop one-directional flow of information from secondary to primary feeders, which can fail to capture the mutual impacts of LV-MV and LV-LV networks on each other, as the distribution grids become more active. 2) Previous joint DSSE methods focus on using the *cloud-based infrastructure* to interconnect the different DSSE levels. Such an infrastructure may impose additional communication costs on utilities. 3) These methods require the system to be completely covered by SMs or pseudo measurements. However, in actual grids, full coverage of SM and high-confidence pseudo-measure generation are rare. 4) Specific SM data quality problems, such as asynchronous errors and missing data, are ignored in these methods, which renders their practical implementation costly. 5) Primary and secondary networks have distinct parametric characteristics. For example, compared to MV systems, the LV networks have higher R/X values and typical branch impedance levels. This characteristic difference between primary and secondary systems can lead to severe ill-conditioning of these joint DSSE solvers.

B. Overall Structure of the Proposed Hierarchical Joint DSSE Framework

In this paper, we have proposed a hierarchical reinforcement learning-aided framework for joint DSSE over primary and secondary distribution systems using customer-side SM data, as shown in Fig. 1. This work presents in detail how to coordinate the hierarchical levels of the SE architecture. Specifically, our framework consists of two layers: at the first layer, a weighted least square (WLS)-based branch current state estimation (BCSE) algorithm is performed over the primary feeder to obtain the states of the MV distribution network, i.e., real/imaginary branch currents. At this layer, all the secondary circuits are treated as aggregated nodes with net equivalent active/reactive power injections provided by the second layer of the hierarchy. Note that, the load data for each secondary node is treated as a variable and estimated using the second

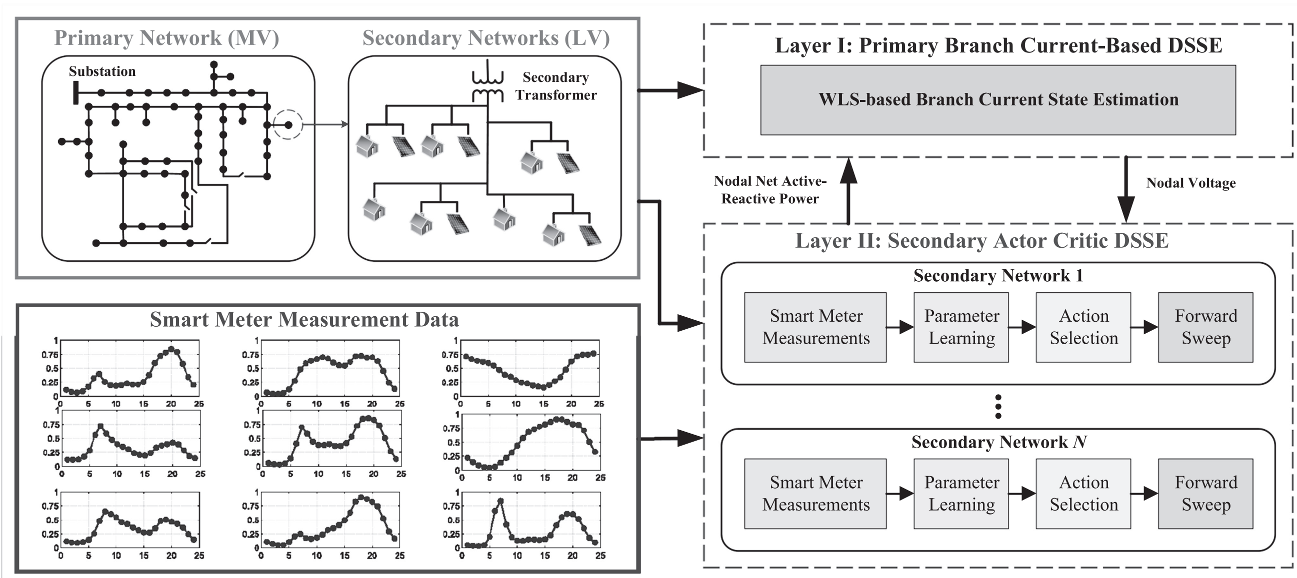

Fig. 1. Reinforcement learning-aided hierarchical DSSE framework.

layer model. Since the WLS is performed only over the primary feeder, it is computationally efficient. After obtaining the states of the primary feeder, the solver passes down the *estimated secondary transformer nodal voltages* to the second layer of the hierarchy. As shown in Fig. 1. This work presents in detail how to coordinate the hierarchical levels of the SE architecture. Specifically, our framework consists of two layers: at the first layer, a weighted least square (WLS)-based branch current state estimation (BCSE) algorithm is performed over the primary feeder to obtain the states of the MV distribution network, i.e., real/imaginary branch currents. At this layer, all the secondary circuits are treated as aggregated nodes with net equivalent active/reactive power injections provided by the second layer of the hierarchy. Note that, the load data for each secondary node is treated as a variable and estimated using the second layer model. Since the WLS is performed only over the primary feeder, it is computationally efficient. After obtaining the states of the primary feeder, the solver passes down the *estimated secondary transformer nodal voltages* to the second layer of the hierarchy.

At the second layer, the estimated transformer nodal voltage is utilized as input to update the nodal load data by solving a machine learning model. Specifically, a deep actor-critic (A-C) module [23] is trained for each LV network of secondary transformers. The goal of the A-C model is to estimate the states of secondary networks (i.e., secondary branch currents) by minimizing the residuals of customer SM voltage measurements. Unlike WLS, the A-C modules leverage their past experiences to adaptively improve their future performance and generalize to unseen situations. The training process takes place offline and the A-C modules are employed online to estimate network states. Thanks to the neural network implementation of the A-C model, the online computation cost is several orders of magnitude lower than that of the WLS method. For each LV secondary network, a nonparametric PDF estimation approach is utilized to generate real and reactive power injections. The OpenDSS software is then leveraged to run power flow analysis. The computed voltages are treated as the voltage measurements, along with the generated load data of the observable customers and secondary transformers' terminal voltages generated at the first layer, used for A-C model offline training. The outputs of the second layer of the hierarchy, which are passed back to the first layer, are the net injected active/reactive powers to the primary feeder for each secondary transformer. These outputs are determined using the A-C-based estimated states of secondary circuits. Hence, the interaction between the two layers of the joint DSSE takes place at the secondary nodes, where nodal voltage flows from the first layer to the second layer and active/reactive power injections are passed in reverse. At each iteration of this closed-loop interaction, each layer revises the states of the network in response to the received inputs from another layer.

The main contributions of our joint DSSE framework can be summarized as follows:

- The proposed method provides comprehensive monitoring of the distribution network at the LV and MV levels. The estimation process has a closed-loop structure to accurately quantify the mutual impacts of primary-secondary networks and secondary-secondary networks on each other.
- Using the proposed A-C method, utilities can achieve a considerable speed-up in solving the joint DSSE in large-scale grids, which allows them to monitor the whole system in real-time. The distributed nature of the proposed framework allows for allocating the computational burdens of DSSE among multiple A-C modules, which further reduces the computation time.
- Compared to the traditional WLS-based method, our deep learning-aided framework eliminates the need for pseudo-measurements to avoid the additional imputation error. The offline training procedure is implemented using simulation data. In addition, our strategy can mitigate the impact of SM data quality issues, including asynchronous errors, missing data, and outliers, on the training process.

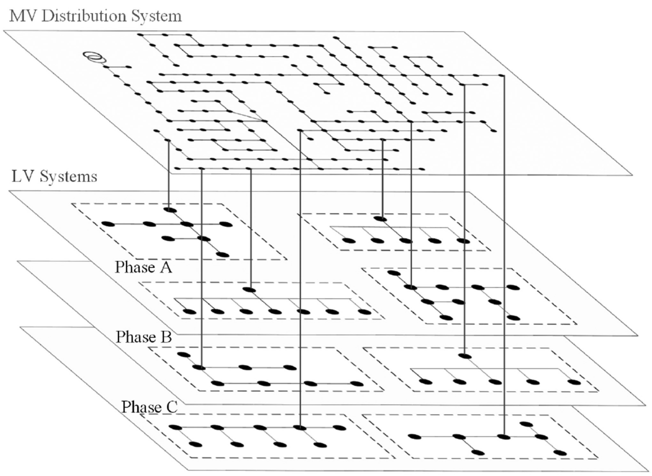

Fig. 2. A three-phase unbalanced MV distribution systems.

- The A-C module allows for explicit learning of the uncertainty of networks' states caused by measurement errors through parametric probabilistic policy functions, which can enhance overall monitoring accuracy.
- The proposed method is able to handle the topology changes in distribution networks. The rationale behind this is that the proposed method only utilizes the deep learning techniques to approximate the secondary-level estimation process. When a topology change occurs on the MV system, the Jacobin matrices in the first layer can be adjusted to accommodate this change.

The rest of the paper is organized as follows: in Section II, the technical details of the proposed hierarchical joint DSSE are presented. In Section III, the numerical results have been analyzed to verify the performance of the joint DSSE method. In Section IV, paper conclusions are presented.

II. Deep Actor-Critic Strategy for Joint DSSE

Fig. 2 shows the common structures of distribution systems at the MV and LV levels. Each LV network is connected to an MV bus by using a single/three-phase transformer. The goal of the proposed method is to provide distribution system situational awareness for both MV and LV networks. In general, our joint DSSE model consists of two parts: an optimization-based solution that infers the system states of the primary-level network, and a deep learning-based method that estimates the customer-level states and provides feedback to the first model. Note that, in this work, the topology and line parameters are considered to be available in a given distribution network. This assumption is realistic and consistent with the recent expansion of smart grid monitoring devices. In some cases without this information, before implementing the proposed method, our previously designed topology and parameter identification method [24] can be applied to obtain complete and accurate system models for MV and LV distribution grids.

A. Primary Network BCSE

At the first layer of the hierarchical joint DSSE, a WLS-based BCSE algorithm is performed over the MV network to minimize the sum of squared residuals (J) [25], [26]. In this paper, vector is in bold.

$$\min_{\boldsymbol{x_p}} J = (\boldsymbol{z_p} - \boldsymbol{h}(\boldsymbol{x_p}))^{\top} W (\boldsymbol{z_p} - \boldsymbol{h}(\boldsymbol{x_p}))$$

$$s.t. \quad \boldsymbol{z_p} = \begin{bmatrix} \boldsymbol{z_{MV}} \\ \boldsymbol{\hat{p}_s} \\ \boldsymbol{\hat{q}_s} \end{bmatrix}$$

$$W = \begin{bmatrix} W_{MV} & \mathbf{0} & \mathbf{0} \\ \mathbf{0} & W_{p_s} & \mathbf{0} \\ \mathbf{0} & \mathbf{0} & W_{q_s} \end{bmatrix} \tag{1}$$

where, $\boldsymbol{x_p}$ is a vector denoting the primary network states, including real and imaginary branch current values, $\boldsymbol{z_p}$ is a vector containing the MV network sensor measurements ($\boldsymbol{z_{MV}}$), including supervisory control and data acquisition (SCADA) and distribution level phasor measurement units (μPMUs), and the estimated total active/reactive power injections of secondary transformers ($\boldsymbol{\hat{p}_s}$, $\boldsymbol{\hat{q}_s}$) that are provided by the second layer of the hierarchy. $\boldsymbol{h}$ is the primary network measurement function that maps state values to measurements. W is a weight matrix that represents the solver's confidence level in each element of $\boldsymbol{z_p}$, which consists of sub-matrices W_{MV}, W_{p_s}, and W_{q_s} corresponding to $\boldsymbol{z_{MV}}$, $\boldsymbol{\hat{p}_s}$, and $\boldsymbol{\hat{q}_s}$, respectively. Here, W_{MV} is determined by the nominal accuracy levels of MV network sensors, e.g., the weight assigned to the measurements received from a specific sensor is selected as the inverse of measurement error variance for that sensor [25]. The elements of W_{p_s}, and W_{q_s} are determined by the estimated uncertainty of the secondary network states as elaborated in Section II-B.

Given the formulation (1), the WLS-based solver performs the following steps to estimate the states of the primary network:

- *Step I:* Receive the latest values of $\boldsymbol{\hat{p}_s}$, $\boldsymbol{\hat{q}_s}$, W_{p_s}, and W_{q_s} from the second layer of the hierarchy (see Section II-B).
- *Step II:* Random state initialization ($\boldsymbol{x_p}[0]$, $k \leftarrow 1$).
- *Step III:* At iteration k, update the measurement function *Jacobian matrix*, H:

$$H = \frac{\partial \boldsymbol{h}(\boldsymbol{x_p}[k-1])}{\partial \boldsymbol{x_p}} \tag{2}$$

  The elements of the Jacobian matrix for the BCSE method can be obtained for arbitrary feeders with known topology. More details of these elements can be referred to [27]. Hence, when the distribution system undergoes reconfiguration, the Jacobin matrix can be easily adjusted to accommodate this change.[1]
- *Step IV:* Update the *gain matrix*, G:

$$G(x) = H^{\top}(\boldsymbol{x_p}[k-1]) W H(\boldsymbol{x_p}[k-1]) \tag{3}$$

- *Step V:* Update the state values using the gain and Jacobian matrices to reduce measurement residuals:

$$\boldsymbol{x_p}[k] = \boldsymbol{x_p}[k-1] + G^{-1} H^{\top} W (\boldsymbol{z_p} - \boldsymbol{h}(\boldsymbol{x_p}[k-1])) \tag{4}$$

[1] Given that the secondary transformers are generally equipped with protection devices, when an outage happens in a radial system, a protective device isolates the faulted area along with the loads downstream of the fault location (i.e., the whole secondary distribution system). In other words, the topology of the secondary distribution systems is typically constant.

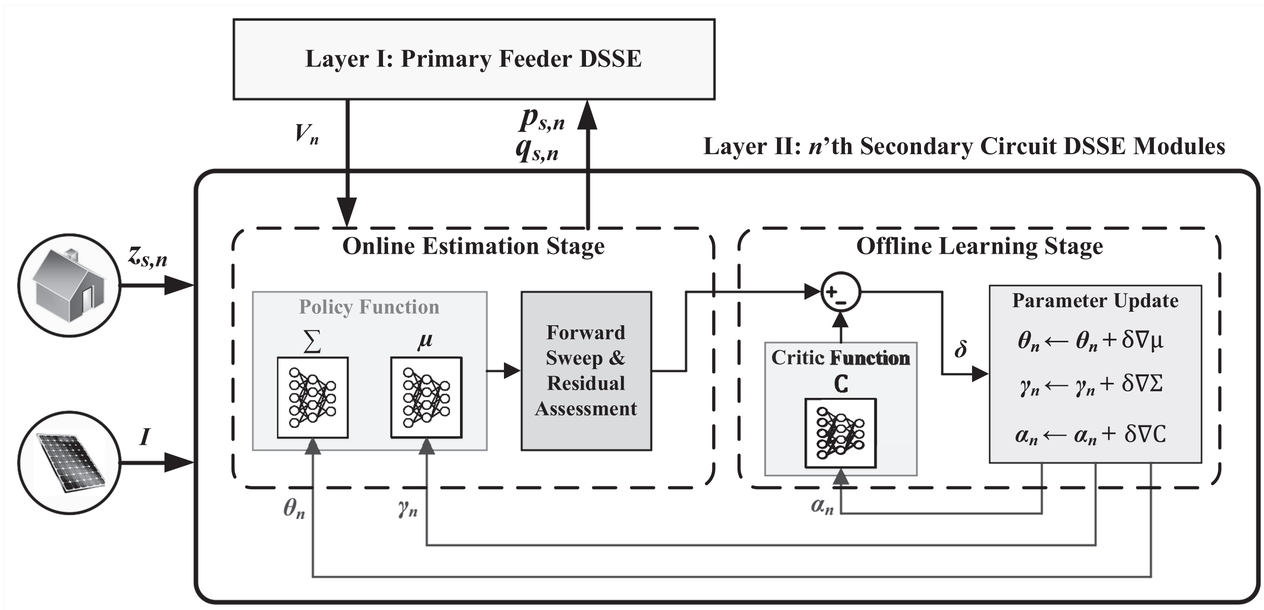

Fig. 3. Layer II: A-C-based DSSE for secondary circuits.

- *Step VI:* $k \leftarrow k+1$; go back to Step III until convergence, i.e., $||\boldsymbol{x_p}[k] - \boldsymbol{x_p}[k-1]|| \leq \delta$, with δ being a user-defined threshold.
- *Step VII:* Given the estimated values of the branches, perform a forward sweep [25] to obtain the voltages of secondary transformers throughout the network. Pass down the estimated voltage of the n'th secondary transformer (V_n) to the corresponding A-C module in the second layer of the joint DSSE hierarchy.

To deal with unbalanced systems, as pointed out in [28], a three-phase distribution line model that considers the self and mutual impedance is used in BCSE. All aforementioned equations still hold. Also, BCSE permits solving coupled and decoupled versions of the WLS by including and ignoring mutual impedances. Compared to traditional state estimation solutions that use node voltages, BCSE adopts branch current as state variables, which is a more natural way of DSSE formulation for distribution systems [2]. The simplification of the measurement functions helps improve computation speed and memory usage. Therefore, BCSE is more suitable for large-scale distribution grids.

B. Reinforcement Learning-Aided State Estimation for Secondary Networks

The computational complexity of the conventional WLS technique is mainly determined by the *matrix inversion*, which induces a complexity of $O((N_{MV}+N_{LV})^3)$. N_{MV} and N_{LV} refer to the number of nodes in the MV and LV system, respectively. In general, $N_{LV} \gg N_{MV}$. Thus, running a BCSE algorithm over the whole primary and secondary networks at the same time is a *computationally intensive* task, especially for large-scale urban systems (i.e., the value of N_{LV} can be in the thousands). To solve this challenge, the second layer of the hierarchy is designed with the objective of simplifying and speeding-up the joint DSSE process to achieve real-time monitoring, as shown in Fig. 3.

Inspired by the recent success of machine learning techniques in the areas of image processing and computer vision, we have leveraged a reinforcement learning technique, the A-C method to handle the low observability problem in real-world distribution systems. Specifically, the A-C parameter learning process takes place offline, and the trained A-C modules are deployed online for fast secondary grid state estimation. For each secondary transformer, an A-C module is trained offline using simulation data. More precisely, following previous works [29]–[31], a nonparametric probability density function (PDF) estimation approach, known as kernel density estimation, is utilized to learn the conditional PDF of customer consumption and PV outputs given the time of the day, using the historical data from observed distribution systems. Such a nonparametric strategy can deal with the non-Gaussian distribution of renewable power. To avoid under-smoothing or over-smoothing issues, a calibration process has been performed to optimize the value of kernel bandwidth by minimizing the overall modeling bias [32]. In some systems without reactive power measurements, empirical load power factors are utilized to calculate the reactive power. Based on the conditional estimated PDFs, a transformation method is then applied to obtain real and reactive data for each customer. By using Monte Carlo simulations, the computed voltages are treated as the voltage measurements, along with the generated net demand data of the observable customers [2] and secondary transformers' terminal voltages generated at the first layer, used for A-C model offline training. Thus, after model training, the

[2]Since residential PVs are typically integrated into distribution systems behind-the-meter, where only the net demand is recorded by SMs. The net demand equals native demand minus the PV generation.

data resource required for online state estimation only include the measurements of the observable customers and the estimated secondary transformers' voltages, which eliminates the need for pseudo-measurements and handles the low observability problem. It should be noted that additional available information, such as high-confidence pseudo-measurements, can also be added to improve the performance of the model, but is not required. One advantage of this training strategy is to mitigate the impact of SM data quality issues, such as asynchronous errors, missing and bad data, on the model development process. Further, in the online application, the proposed method can be easily integrated with previous data recovery methods to address the SM data quality problems [33], [34].

As detailed below, the A-C module is a combination of policy-based and value-based reinforcement learning, which has advantages from both. Specifically, A-C module consists of two deep learning components that are trained cooperatively: (1) the *actor* represents the secondary state estimation *policy function* (π_n), which receives external inputs for the n'th secondary circuit, including the SM voltage/energy measurements ($\boldsymbol{z}_{s,n}$), and the estimated transformer voltage from the first layer (V_n), and maps them to secondary states, $\boldsymbol{x}_{s,n}$. Here, $\boldsymbol{x}_{s,n}$ are the real/imaginary components of secondary circuit branch currents. This mapping is formulated as a D_n-dimensional parametric multivariate Gaussian probability distribution function, where $\boldsymbol{x}_{s,n} \in \mathbb{R}^{D_n}$ [35]:

$$\begin{aligned}\boldsymbol{x}_{s,n} &\sim \pi_n(\boldsymbol{\mu_n}, \Sigma_n)\\ &= \frac{1}{\sqrt{|\Sigma_n|(2\pi)^{D_n}}} e^{-\frac{1}{2}(\boldsymbol{x}_{s,n}-\boldsymbol{\mu_n})^\top \Sigma_n^{-1}(\boldsymbol{x}_{s,n}-\boldsymbol{\mu_n})}\end{aligned} \quad (5)$$

where, $\boldsymbol{c}_n = [\boldsymbol{z}_{s,n}\ V_n]$, and $\boldsymbol{\mu_n}$ and Σ_n are the n'th secondary circuit state mean vector and covariance matrix, respectively. In this paper, these two statistical factors are parameterized using two deep neural networks (DNNs), $\mathcal{A}_\mu$ and $\mathcal{A}_\Sigma$, with parameters $\boldsymbol{\theta_n}$ and $\boldsymbol{\gamma_n}$:

$$\boldsymbol{\mu}_n = \mathcal{A}_\mu(\boldsymbol{c}_n|\boldsymbol{\theta_n}) \quad (6)$$

$$\Sigma_n = \mathcal{A}_\Sigma(\boldsymbol{c}_n|\boldsymbol{\gamma_n}) \quad (7)$$

Basically, parameters $\boldsymbol{\theta_n}$ and $\boldsymbol{\gamma_n}$ are the weight and biases assigned to the synapses in the DNNs, which need to be learned. This enables the operator to accurately quantify, not only the expected value of the secondary circuit states, but also their uncertainty, which is a critical element in grids with high renewable penetration. (2) The *critic* is a DNN denoted by $\mathcal{C}$ with parameters $\boldsymbol{\alpha_n}$ for the n'th circuit, which quantifies how well the actor is performing. In our problem, the critic tries to predict the secondary network estimation residuals based on the inputs to the second layer:

$$\hat{r}_n = \mathcal{C}(\boldsymbol{c}_n|\boldsymbol{\alpha_n}) \quad (8)$$

where, $\hat{r}_n$ represents the approximate residuals; ideally, if the critic has perfect performance, then, $\hat{r}_n = r_n$, meaning that the predicted residuals are equal to the realized measurement residuals r_n.

Given the defined A-C modules, the computational process at the second layer of the hierarchy consists of a state estimation stage (A), which is performed jointly with the first layer, and a parameter update stage (B), which is confined to the second layer alone.

- *Stage A - [Joint DSSE]*
- *Step A-I:* Input the learned A-C parameters $\boldsymbol{\theta_n}, \boldsymbol{\gamma_n}$, and $\boldsymbol{\alpha_n}$.
- *Step A-II:* Receive the updated V_n from the first layer, and construct the external input vector, $\boldsymbol{c}_n$.
- *Step A-III:* Construct the policy function π_n, according to (5), using parameters $\boldsymbol{\theta_n}$ and $\boldsymbol{\gamma_n}$ and external inputs $\boldsymbol{c}_n$.
- *Step A-IV:* Sample secondary circuit states in real-time using the constructed policy function, $\boldsymbol{x}_{s,n} \leftarrow \pi_n$.
- *Step A-V:* Use generated states to perform a forward sweep [25] over the secondary circuit to obtain the net active/reactive power injections at the transformer node, $\hat{p}_{s,n}$ and $\hat{q}_{s,n}$, as follows:

$$\hat{p}_{s,n} = V_n I_{Re,n} \quad (9)$$

$$\hat{q}_{s,n} = V_n I_{Im,n} \quad (10)$$

where, $I_{Re,n} \in \boldsymbol{x}_{s,n}$ and $I_{Im,n} \in \boldsymbol{x}_{s,n}$ are the estimated net real and imaginary current components of n'th secondary transformer.
- *Step A-VI:* To construct W_{p_s} and W_{q_s}, the variances of $\hat{p}_{s,n}$ and $\hat{q}_{s,n}$ need to be obtained. Noting that the uncertainty of LV circuits states are explicitly quantified by the covariance matrix of the policy function, π_n, we have:

$$\sigma^2_{p_{s,n}} = (V_n)^2 \Sigma_{I_{Re,n}} \quad (11)$$

$$\sigma^2_{q_{s,n}} = (V_n)^2 \Sigma_{I_{Im,n}} \quad (12)$$

where, $\sigma^2_{p_{s,n}}$ and $\sigma^2_{q_{s,n}}$ are the variances of the net active and reactive power for the n'th LV system, and $\Sigma_{I_{Re,n}}$ and $\Sigma_{I_{Im,n}}$ are components of Σ_n corresponding to the states $I_{Re,n}$ and $I_{Im,n}$, respectively. These variables are determined using $\mathcal{A}_\Sigma(\boldsymbol{c}_n|\boldsymbol{\gamma_n})$. Therefore, the weights assigned to $p_{s,n}$ and $q_{s,n}$ in the WLS-based solver of layer I are equal to $\sigma^{-2}_{p_{s,n}}$ and $\sigma^{-2}_{q_{s,n}}$, respectively.
- *Step A-VII:* Pass the net active/reactive power injection of all secondary transformers to the first layer of the joint DSSE framework, $\hat{\boldsymbol{p}}_{\boldsymbol{s}} = [\hat{p}_{s,1}, \ldots, \hat{p}_{s,N}]$ and $\hat{\boldsymbol{q}}_{\boldsymbol{s}} = [\hat{q}_{s,1}, \ldots, \hat{q}_{s,N}]$. Go back to Step A-II until V_n is stabilized.
- *Stage B - [A-C Parameter Update]*
- *Step B-I:* After the state estimation process has converged, re-sample states using the latest policy function, $\boldsymbol{x}_{s,n} \leftarrow \pi_n + \boldsymbol{u_n}$, where $\boldsymbol{u_n}$ is a *exploratory perturbation* generated using a zero-mean uniform distribution. This perturbation allows the A-C module to actively search for potential improvements in the learned policy and escape local minimums.
- *Step B-II:* Estimate the secondary DSSE residuals from the critic, using $\boldsymbol{c}_n$ and DNN parameters $\boldsymbol{\alpha_n}$, according to (8).
- *Step B-III:* Use generated state sample and the latest value of V_n from Step A-VII, to perform a forward sweep over the secondary circuit to obtain the estimated voltages; use the estimated nodal voltages to obtain the realized residual, r_n.
- *Step B-IV:* Obtain the *temporal difference error* (TDE), $\delta_n = r_n - \hat{r}_n$, and use it to update the parameters of the

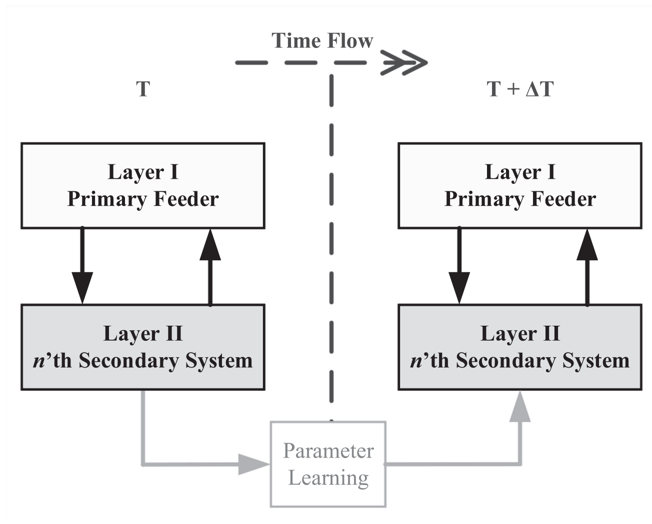

Fig. 4. Temporal function of the proposed hierarchical joint DSSE.

critic:

$$\boldsymbol{\alpha_n} \leftarrow \boldsymbol{\alpha_n} + l_c \delta_n \nabla_{\boldsymbol{\alpha_n}} \mathcal{C}(\boldsymbol{c}_n) \tag{13}$$

where, l_c is a learning rate, and $\nabla_{\boldsymbol{\alpha_n}} \mathcal{C}$ is the gradient of the critic DNN with respect to its parameters. This computation is performed using back-propagation over the DNN [23].

- *Step B-V:* Update the parameters of the actor, using the TDE:

$$\boldsymbol{\theta_n} \leftarrow \boldsymbol{\theta_n} + l_a \delta_n \boldsymbol{u_n} \nabla_{\boldsymbol{\theta_n}} \pi_n(\boldsymbol{c}_n) \tag{14}$$

$$\boldsymbol{\gamma_n} \leftarrow \boldsymbol{\gamma_n} + l_a \delta_n \boldsymbol{u_n} \nabla_{\boldsymbol{\gamma_n}} \pi_n(\boldsymbol{c}_n) \tag{15}$$

with l_a denoting the rate of policy learning. To obtain the gradient of policy function with respect to DNN parameters, $[\boldsymbol{\theta_n}, \boldsymbol{\gamma_n}]$, chain rule is applied to the two sets of parameters separately:

$$\nabla_{\boldsymbol{\theta_n}} \pi(\boldsymbol{c}_n) = \frac{\Sigma_n^{-1}(\boldsymbol{x}_{s,n} - \boldsymbol{\mu}_n)}{\sqrt{|\Sigma_n|(2\pi)^{D_n}}} e^{-\frac{M}{2}} \nabla_{\boldsymbol{\theta_n}} \mathcal{A}_\mu(\boldsymbol{c}_n) \tag{16}$$

$$\begin{aligned} &\nabla_{\boldsymbol{\gamma_n}} \pi(\boldsymbol{c}_n) \\ &= \frac{-\Sigma_n^{-1}(I - (\boldsymbol{x}_{s,n} - \boldsymbol{\mu}_n)(\boldsymbol{x}_{s,n} - \boldsymbol{\mu}_n)^\top \Sigma_n^{-1}) e^{-\frac{M}{2}}}{2\sqrt{|\Sigma_n|(2\pi)^{D_n}}} \\ &\nabla_{\boldsymbol{\gamma_n}} \mathcal{A}_\Sigma(\boldsymbol{c}_n) \end{aligned} \tag{17}$$

where, $M = (\boldsymbol{c_n} - \boldsymbol{\mu}_n)^\top \Sigma_n^{-1} (\boldsymbol{c_n} - \boldsymbol{\mu}_n)$ is an auxiliary matrix. Note that $\nabla_{\boldsymbol{\theta_n}} \mathcal{A}_\mu$ and $\nabla_{\boldsymbol{\gamma_n}} \mathcal{A}_\Sigma$ in (16) and (17) are obtained using back-propagation over the two DNNs of the actor.

- *Step B-VI:* Move to the next time-step; go back to Step A-I.

Fig. 4 shows the temporal functionality of the proposed A-C method. As can be seen, the parameters of DNNs are updated and replaced across time steps, while on the other hand, the bi-layer estimation takes place at each time step given the latest values of parameters. This enables the hierarchical framework to adapt to changes in the feeder across time, while offering fast real-time monitoring capability to utilities. Thus, in rare cases with secondary topology changes, the proposed method can continuously update the parameters of both DNNs to adapt to the new topology. Unlike most supervised learning-based DSSE methods that require retraining DNNs for new topologies, our approach provides a low-cost solution for topology change in both primary and secondary networks.

C. Convergence Analysis

The two layers of our model continuously exchange boundary information, including transformer voltages (first layer to second layer) and active/reactive total power injection (second layer to first layer). A major challenge in this model is to ensure the convergence of system monitoring, especially at the earlier stage of training when unreliable estimates generated by A-C modules may cause numerical instability for WLS. To avoid this, we have designed a confidence weight-based strategy. The basic idea is to integrate the TDE from the second layer (i.e., A-C modules) into the confidence matrix of the first layer (i.e., WLS). The TDE is able to measure how well the DNNs infer system states over time, which is a good metric for determining the reliability of the estimated secondary network states. Therefore, the A-C modules with lower TDE will receive higher confidence weights at the WLS. Also, as we mentioned before, the A-C modules are pre-trained using simulation data, which further reduces the risk of numerical instability during online estimation.

III. Numerical Results

This section explores the practical performance of our joint DSSE framework. As detailed below, the test system for this case study is a three-phase unbalanced distribution feeder that consists of a 60-node 13.8 kV primary feeder and 44 secondary circuits with a total number of 238 customers from a utility partner in the U.S. The topology of the primary feeder and two exemplary secondary networks are shown in Fig. 5. The real SCADA/SM data and MV-LV network OpenDSS models of this distribution feeder are utilized to verify our method. The data includes customers' energy/voltage measurements at the secondary networks, and total primary feeder active/reactive power and substation voltages. More details on the data are available online [36]. It should be noted that these real-world measurement data is naturally imperfect. According to our utility partners, an error tolerance of $\pm 1\%$ can be expected. In addition, to further validate our method under noisy conditions, error samples were generated from a normal distribution with zero mean and 1% variance and added to the voltage values obtained from the OpenDSS simulator to represent standard measurement deviations [15].

To validate our hierarchical reinforcement learning-aided DSSE framework, we have assumed that 30% of the customers are randomly selected to install SMs in this feeder. This assumption is consistent with the number of recently reported SMs in the U.S.[3]. The locations of SMs are randomly selected. Distributed solar resources are added to the secondary networks to capture the impact of uncertain renewable resources on DSSE.

[3]By the end of 2020, an estimated 107 million SMs were deployed with an annual growth of 8 million devices from the previous year [37]. These SMs cover about 75% of U.S. households.

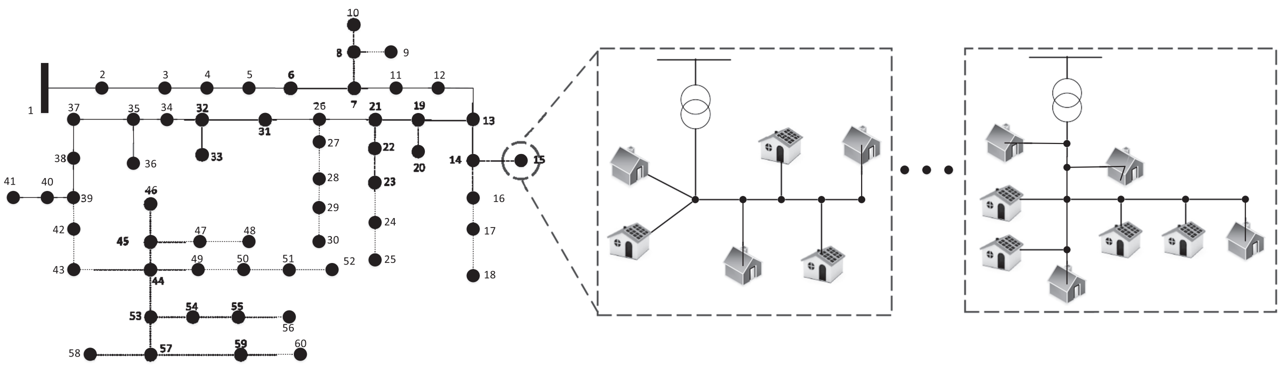

Fig. 5. Test feeder topology and secondary network examples.

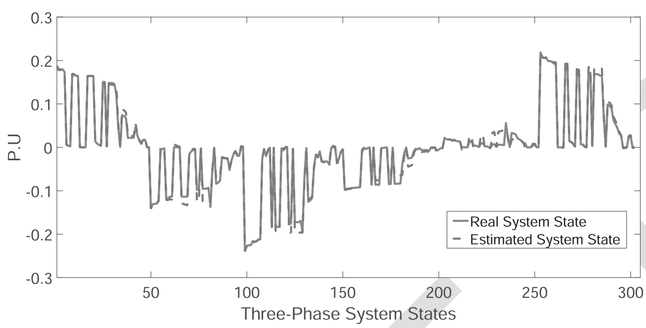

Fig. 6. Comparison of estimated system states and real values.

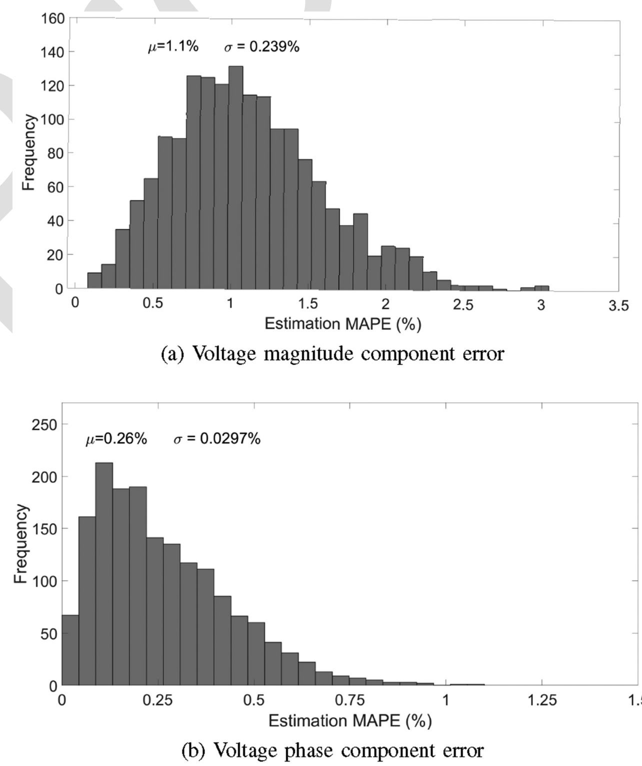

Fig. 7. Voltage magnitude and phase estimation using the proposed reinforcement learning-aided hierarchical DSSE model.

The penetration level of renewable power is 50% with respect to the long-term average peak load. The solar power data is adopted from [38]. In DSSE, the maximum error values for the real measurements is 3%. In this work, the hyperparameter set of the A-C modules is calibrated by using the random search strategy [39]. As a result, the three DNNs, $\mathcal{A}_\mu$, $\mathcal{A}_\Sigma$, and $\mathcal{C}$, consist of 3 hidden layers of 10 neurons. The learning rates of actor and critic, l_a and l_c, are selected as 0.01 based on the performance of the validation process.

A. The Performance of the Proposed Joint DSSE Method

The A-C module is trained for various secondary networks in parallel based on the simulation data and tested using the new data inquiry. In this experiment, for each LV network, the number of training data is 1000. After model training, Fig. 6 compares the estimated primary-level distribution system states (i.e., branch current real and imaginary parts) with the actual state values using the proposed method at a specific time point. As is demonstrated in the figure, the outcome of our method closely follows the underlying states. It should be noted that our test network is a three-phase unbalanced distribution system and the phase connections of customers are known. Furthermore, to validate the average performance of the proposed method, we have tested our method over a long-term period (more than 1500 time points). The error distribution is shown in Fig. 7. The Mean Absolute Percentage Error (MAPE) criterion is used here to evaluate the accuracy of state estimation:

$$M = \frac{100\%}{n_s} \sum_{t=1}^{n_s} \left| \frac{\hat{A(t)} - A(t)}{\hat{A(t)}} \right| \tag{18}$$

where, $\hat{A(t)}$ and $A(t)$ are the actual state value and the estimated value. As is demonstrated in these figures, the estimation errors for voltage magnitude and phase angle are 1.1% and 0.26%, respectively. These results corroborate the satisfactory performance of the proposed model over real data.

Although our A-C-aided DSSE method can eliminate the need for pseudo-measurement generation, the system observability (i.e., SM penetration ratio) still impacts its performance due to information loss. To demonstrate the sensitivity of the joint

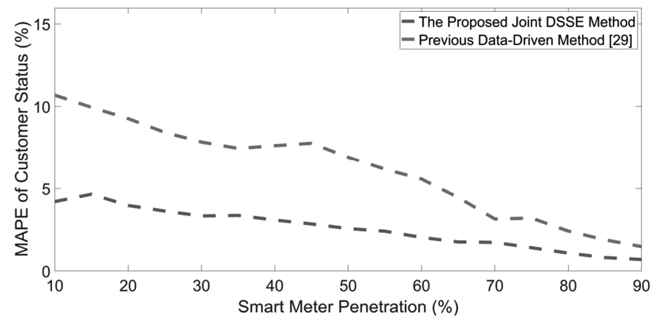

Fig. 8. Sensitivity analysis: quantifying the impact of observability (i.e., smart meter penetration) on state estimation accuracy.

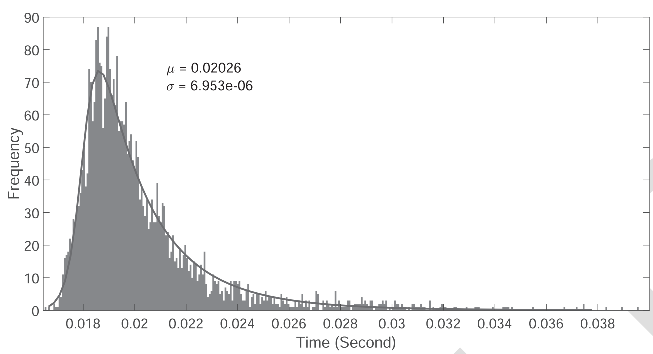

(a) Probability density function of online action selection time

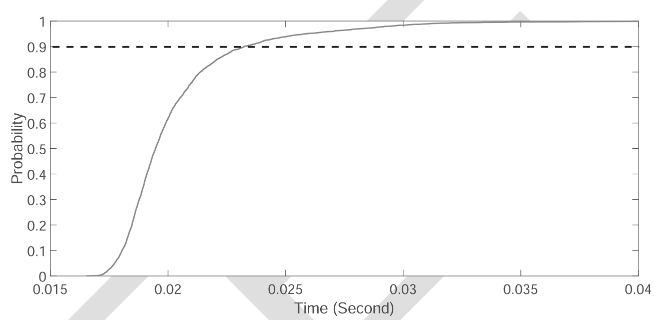

(b) Cumulative distribution function of online action selection time

Fig. 9. Statistical results of online action selection time.

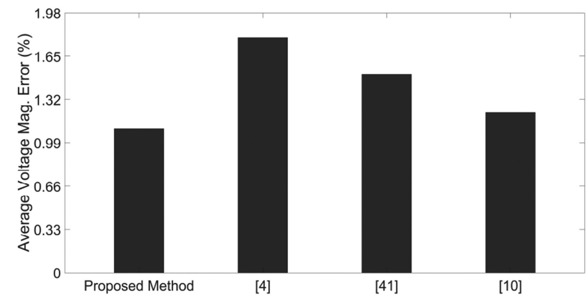

(a) Comparison of voltage magnitude component errors

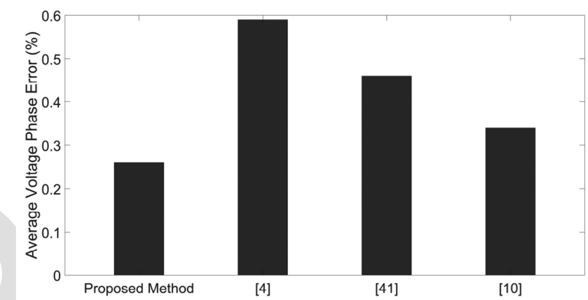

(b) Comparison of voltage phase component errors

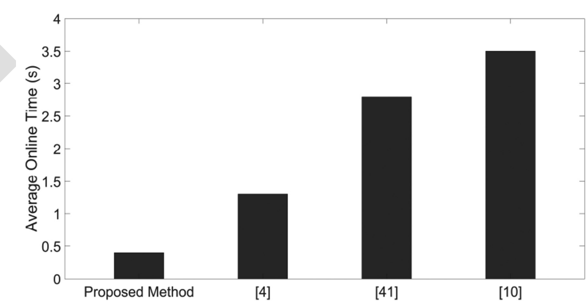

(c) Comparison of online computation

Fig. 10. Comparison results between [4], [10], [40], and the proposed method.

DSSE accuracy to the system observability, Fig. 8 shows the secondary-level state estimation accuracy of the proposed method under various SM penetration ratios by calculating estimation errors for voltage magnitude and phase angle. SM penetration is determined by the number of customers and SMs. In this figure, the blue dashed line describes the state estimation accuracy of the proposed method under various SM penetration levels by calculating estimation errors for voltage magnitude and phase angle. When the system observability is only 10%, the error is around 5%. When the system observability is 50%, the error is around 2%. Also, the accuracy of a previous machine learning-based method is compared with our solution, as shown by the red dashed line [29]. Based on the results of the two data-driven methods, it is clear that the state estimation accuracy decreases as the percentage of SM penetration decreases. Thanks to its hierarchical nature, in this case, our method outperforms the existing learning-based method at all observability levels. Also, these results show that the proposed method can provide a comprehensive and accurate monitoring of the distribution network at the LV and MV levels.

B. Method Comparison

To further demonstrate the performance of the proposed joint DSSE framework, we have conducted numerical comparisons with three state-of-the-art methods, including a multi-area DSSE method [4], a hybrid framework [40], and an optimization-based solution [10]. The three methods are simulated with the same real-world datasets to calculate the accuracy of the methods. The comparison results are shown in 10. As demonstrated in the figure, in terms of voltage magnitude, the average estimation errors are 1.1%, 1.79$, 1.51%, and 1.22% for the proposed solution, [4], [40] and [10], respectively. In terms of voltage phase angle, the average estimation errors are 0.26%, 0.59%, 0.46%, and 0.34%, respectively. In terms of online computation

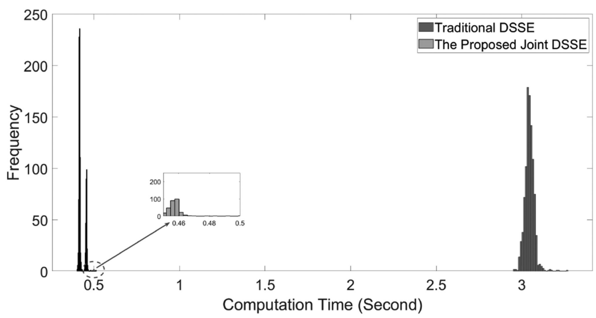

Fig. 11. Computation time comparisons (the proposed actor-critic-based method versus the traditional optimization-based method).

complexity, the average times are 0.4 seconds, 1.3 seconds, 2.8 seconds, and 3.5 seconds, respectively. A few observations follow: (1) The traditional optimization-based method (i.e., [4]) is more likely to be affected by the high penetration of renewable power resources than methods incorporating machine learning techniques, thus reducing accuracy. The rationale behind this is that it is hard to find a good heuristic initial guess due to the fast changes in the system states. (2) Among the machine learning-based methods, the proposed solution can achieve a better performance compared to the previous works. (3) Even though previous method (i.e., [10]) can be extended to a unified model of all primary and secondary circuits for comprehensive system monitoring, this extension leads to a significant increase in computational burden. (4) Compared with the multi-area and the hybrid methods (i.e., [4] and [40]), the proposed method decomposes monitoring into two interconnected layers and then limits Jacobian matrix computations to the primary feeders, thus significantly accelerating real-time monitoring. This comparison result demonstrates the competitiveness of our solution.

C. Computational Complexity Analysis

To ensure that the proposed method can provide real-time monitoring in practice, we have tracked the computation time. Note that the case study is conducted on a standard PC with an Intel(R) Xeon(R) CPU running at 3.70 GHz and with 32.0 GB of RAM. Fig. 9 presents the computation time distribution of the online action selection of A-C modules. Considering the uncertainty of the computation speed, 3500 Monte Carlo simulations have been performed. As shown in the figure, the majority of online action time are concentrated around 0.02 s. Moreover, based on the cumulative distribution function of online action time, almost 90% of simulations have online action time below 0.024 seconds, thus ensuring real-time system monitoring. Moreover, the computation time of the whole hierarchical framework is tested and compared to the WLS-based method [27]. Fig. 11 shows the computation time distributions of our proposed method and an existing monitoring model [27] over a 60-node distribution network. As can be observed, the computation time is reduced from about 3 seconds to about 0.5 seconds. In this case, our framework is able to significantly improve the computation time by an average factor of 6 times. It should be noted that our test system is a middle-size rural distribution feeder that has a limited number of customers. Since the computation burden of the optimization method grows exponentially, our method's improvements in computation time would be higher in large-scale urban systems. Such low computational complexity also can help handle significant system state shift caused by distributed energy resources and plug-in electric vehicles in a short period of time [20]. Consequently, our joint DSSE solver can truly reflect the operating point of the modern distribution system.

IV. Conclusion

In this paper, we have presented a reinforcement learning-aided hierarchical DSSE solution to jointly monitor the primary and secondary distribution networks. Compared to previous works, the proposed solution is scalable to large grids and can accurately capture the impact of volatile grid-edge renewable resources on system states. Our model enables fast online estimation of secondary network states, while allowing for offline evaluation and updates of DNNs. Further, the proposed method can eliminate the need for pseudo-measurements and reduce the impact of data quality issues. The hierarchical joint DSSE method has been tested using real SM data and models of distribution grids. It is observed that after the estimation policy function is fully learned, the proposed method can accurately estimate the primary and secondary system states. Moreover, the results show that this solution is able to outperform previous monitoring methods in terms of estimation accuracy and computation time.

References

[1] V. Zamani and M. Baran, "Feeder monitoring for Volt/VAR control in distribution systems," in *Proc. IEEE PES Gen. Meeting (Conf. Expo.)*, 2014, pp. 1–5.
[2] K. Dehghanpour, Z. Wang, J. Wang, Y. Yuan, and F. Bu, "A survey on state estimation techniques and challenges in smart distribution systems," *IEEE Trans. Smart Grid*, vol. 10, no. 2, pp. 2312–2322, Mar. 2019.
[3] P. A. Pegoraro *et al.*, "Bayesian approach for distribution system state estimation with non-Gaussian uncertainty models," *IEEE Trans. Instrum. Meas.*, vol. 66, no. 11, pp. 2957–2966, Nov. 2017.
[4] M. Pau, F. Ponci, A. Monti, S. Sulis, C. Muscas, and P. A. Pegoraro, "An efficient and accurate solution for distribution system state estimation with multiarea architecture," *IEEE Trans. Instrum. Meas.*, vol. 66, no. 5, pp. 910–919, May 2017.
[5] J. Wu, Y. He, and N. Jenkins, "A robust state estimator for medium voltage distribution networks," *IEEE Trans. Power Syst.*, vol. 28, no. 2, pp. 1008–1016, May 2013.
[6] F. Therrien, I. Kocar, and J. Jatskevich, "A unified distribution system state estimator using the concept of augmented matrices," *IEEE Trans. Power Syst.*, vol. 28, no. 3, pp. 3390–3400, Aug. 2013.
[7] A. Gomez-Exposito, C. Gomez-Quiles, and I. Dzafic, "State estimation in two time scales for smart distribution systems," *IEEE Trans. Smart Grid*, vol. 6, no. 1, pp. 421–430, Jan. 2015.
[8] B. P. Hayes, J. K. Gruber, and M. Prodanovic, "A closed-loop state estimation tool for MV network monitoring and operation," *IEEE Trans. Smart Grid*, vol. 6, no. 4, pp. 2116–2125, Jul. 2015.
[9] A. Al-Wakeel, J. Wu, and N. Jenkins, "State estimation of medium voltage distribution networks using smart meter measurements," *Appl. Energy*, vol. 184, pp. 207–218, Dec. 2016.
[10] Y. Zhang, J. Wang, and Z. Li, "Interval state estimation with uncertainty of distributed generation and line parameters in unbalanced distribution systems," *IEEE Trans. Power Syst.*, vol. 35, no. 1, pp. 762–772, Jan. 2020.
[11] Y. Chen, Y. Yao, and Y. Zhang, "A robust state estimation method based on SOCP for integrated electricity-heat system," *IEEE Trans. Smart Grid*, vol. 12, no. 1, pp. 810–820, Jan. 2021.

[12] D. A. Haughton and G. T. Heydt, "A linear state estimation formulation for smart distribution systems," *IEEE Trans. Power Syst.*, vol. 28, no. 2, pp. 1187–1195, May 2013.
[13] A. Angioni, T. Schlosser, F. Ponci, and A. Monti, "Impact of pseudo-measurements from new power profiles on state estimation in low-voltage grids," *IEEE Trans. Instrum. Meas.*, vol. 65, no. 1, pp. 70–77, Jan. 2016.
[14] M. Huang, Z. Wei, M. Pau, F. Ponci, and G. Sun, "Interval state estimation for low-voltage distribution systems based on smart meter data," *IEEE Trans. Instrum. Meas.*, vol. 68, no. 9, pp. 3090–3099, Sep. 2019.
[15] A. Abdel-Majeed and M. Braun, "Low voltage system state estimation using smart meters," in *Proc. 47th Int. Univ. Power Eng. Conf.*, 2012, pp. 1–6
Q3 [16] A. Mutanen, S. Repo, P. Järventausta, A. Löf, and D. D. Giustina, "Testing low voltage network state estimation in RTDS environment," in *Proc. IEEE PES ISGT Europe*, 2013, pp. 1–5.
[17] M. Pertl, K. Heussen, O. Gehrke, and M. Rezkalla, "Voltage estimation in active distribution grids using neural networks," in *Proc. IEEE Power Energy Soc. Gen. Meeting*, 2016, pp. 1–5.
[18] R. Bessa, G. Sampaio, V. Miranda, and J. Pereira, "Probabilistic low-voltage state estimation using analog-search techniques," in *Proc. Power Syst. Comput. Conf.*, 2018, pp. 1–7.
[19] D. Waeresch, R. Brandalik, W. H. Wellssow, J. Jordan, R. Bischler, and N. Schneider, "Linear state estimation in low voltage grids based on smart meter data," in *Proc. IEEE Eindhoven PowerTech*, 2015, pp. 1–6.
[20] Y. Weng, R. Negi, C. Faloutsos, and M. D. Ilić, "Robust data-driven state estimation for smart grid," *IEEE Trans. Smart Grid*, vol. 8, no. 4, pp. 1956–1967, Jul. 2017.
[21] M. Pau *et al.*, "A cloud-based smart metering infrastructure for distribution grid services and automation," *Sustain. Energy, Grids Netw.*, vol. 15, pp. 14–25, Sep. 2018.
[22] M. Pau *et al.*, "Design and accuracy analysis of multilevel state estimation based on smart metering infrastructure," *IEEE Trans. Instrum. Meas.*, vol. 68, no. 11, pp. 4300–4312, Nov. 2019.
[23] I. Grondman, M. Vaandrager, L. Busoniu, R. Babuska, and E. Schuitema, "Efficient model learning methods for actor-critic control," *IEEE Trans. Syst., Man, Cybern. B., Cybern*, vol. 42, no. 3, pp. 591–602, Jun. 2012.
[24] Y. Guo, Y. Yuan, and Z. Wang, "Distribution grid modeling using smart meter data," *IEEE Trans. Power Syst.*, to be published, doi: 10.1109/TPWRS.2021.3118004.
[25] M. E. Baran and A. W. Kelley, "A branch-current-based state estimation method for distribution systems," *IEEE Trans. Power Syst.*, vol. 10, no. 1, pp. 483–491, Feb. 1995.
Q4 [26] R. Singh, B. Pal, and R. A. Jabr, "Choice of estimator for distribution system state estimation," *IET Gener. Transmiss. Distrib.*, vol. 3, pp. 666–678, 2009.
[27] H. Wang and N. N. Schulz, "A revised branch current-based distribution system state estimation algorithm and meter placement impact," *IEEE Trans. Power Syst.*, vol. 19, no. 1, pp. 207–213, Feb. 2004.
[28] M. Pau, P. A. Pegoraro, and S. Sulis, "Efficient branch-current-based distribution system state estimation including synchronized measurements," *IEEE Trans. Instrum. Meas.*, vol. 62, no. 9, pp. 2419–2429, Sep. 2013.
[29] K. R. Mestav, J. Luengo-Rozas, and L. Tong, "Bayesian state estimation for unobservable distribution systems via deep learning," *IEEE Trans. Power Syst.*, vol. 34, no. 6, pp. 4910–4920, Nov. 2019.
[30] W. Zhou, O. Ardakanian, H. Zhang, and Y. Yuan, "Bayesian learning-based harmonic state estimation in distribution systems with smart meter and DPMU data," *IEEE Trans. Smart Grid*, vol. 11, no. 1, pp. 832–845, Jan. 2020.
[31] Y. Yuan, K. Dehghanpour, F. Bu, and Z. Wang, "A probabilistic data-driven method for photovoltaic pseudo-measurement generation in distribution systems," in *Proc. IEEE Power Energy Soc. Gen. Meeting*, 2019, pp. 1–5.
[32] P. Pinson, H. A. Nielsen, J. K. Moller, H. Madsen, and G. Kariniotakis, "Nonparametric probabilistic forecasts of wind power: Required properties and evaluation," *Wind Energy*, vol. 10, no. 6, pp. 497–516, Nov. 2007.
[33] F. Ni, P. H. Nguyen, J. F. G. Cobben, H. E. van den Brom, and D. Zhao, "Uncertainty analysis of aggregated smart meter data for state estimation," in *Proc. IEEE Int. Workshop Appl. Meas. Power Syst.*, 2016, pp. 1–6.
[34] Y. Yuan, K. Dehghanpour, and Z. Wang, "Mitigating smart meter asynchrony error via multi-objective low rank matrix recovery," *IEEE Trans. Smart Grid*, vol. 12, no. 5, pp. 4308–4317, Sep. 2021.
[35] Y. Wei, F. R. Yu, M. Song, and Z. Han, "User scheduling and resource allocation in hetnets with hybrid energy supply: An actor-critic reinforcement learning approach," *IEEE Trans. Wireless Commun.*, vol. 17, no. 1, pp. 680–692, Jan. 2018.
[36] F. Bu, Y. Yuan, Z. Wang, K. Dehghanpour, and A. Kimber, "A time-series distribution test system based on real utility data," 2019, *arXiv:1906.04078*.
[37] Institute for Electric Innovation, "Electric company smart meter deployments: Foundation for a smart grid," Apr. 2021.
[38] C. Holcomb, "Pecan street inc.: A test-bed for nilm," 2012. [Online]. Available: https://www.pecanstreet.org/
[39] J. Bergstra and Y. Bengio, "Random search for hyper-parameter optimization," *J. Mach. Learn. Res.*, vol. 13, pp. 281–305, Feb. 2012.
[40] A. S. Zamzam, X. Fu, and N. D. Sidiropoulos, "Data-driven learning-based optimization for distribution system state estimation," *IEEE Trans. Power Syst.*, vol. 34, no. 6, pp. 4796–4805, Nov. 2019.

Yuxuan Yuan (Graduate Student Member, IEEE) received the B.S. degree in electrical & computer engineering in 2017 from Iowa State University, Ames, IA, USA, where he is currently working toward the Ph.D. degree. His research interests include distribution system state estimation, synthetic networks, data analytics, and machine learning.

Kaveh Dehghanpour received the B.Sc. and M.S. degrees in electrical and computer engineering from the University of Tehran, Tehran, Iran, in 2011 and 2013, respectively, and the Ph.D. degree in electrical engineering from Montana State University, Bozeman, MT, USA, in 2017. He is currently a Postdoctoral Research Associate with Iowa State University, Ames, IA, USA. His research interests include application of machine learning and data-driven techniques in power system monitoring and control.

Zhaoyu Wang (Senior Member, IEEE) received the B.S. and M.S. degrees in electrical engineering from Shanghai Jiaotong University, Shanghai, China, and the M.S. and Ph.D. degrees in electrical and computer engineering from the Georgia Institute of Technology, Atlanta, GA, USA. He is the Northrop Grumman Endowed Associate Professor with Iowa State University, Ames, IA, USA. His research interests include optimization and data analytics in power distribution systems and microgrids. He was the recipient of the National Science Foundation CAREER Award, the Society-Level Outstanding Young Engineer Award from IEEE Power and Energy Society (PES), the Northrop Grumman Endowment, College of Engineering's Early Achievement in Research Award, and the Harpole-Pentair Young Faculty Award Endowment. He is the Principal Investigator for a multitude of projects funded by the National Science Foundation, Department of Energy, National Laboratories, PSERC, and Iowa Economic Development Authority. He is the Chair of IEEE PES PSOPE Award Subcommittee, Co-Vice Chair of PES Distribution System Operation and Planning Subcommittee, and the Vice Chair of PES Task Force on Advances in Natural Disaster Mitigation Methods. He is an Associate Editor for the IEEE TRANSACTIONS ON POWER SYSTEMS, IEEE TRANSACTIONS ON SMART GRID, IEEE OPEN ACCESS JOURNAL OF POWER AND ENERGY, IEEE POWER ENGINEERING LETTERS, and *IET Smart Grid*.

Fankun Bu (Graduate Student Member, IEEE) received the B.S. and M.S. degrees from North China Electric Power University, Baoding, China, in 2008 and 2013, respectively. He is currently working toward the Ph.D. degree with the Department of Electrical and Computer Engineering, Iowa State University, Ames, IA, USA. From 2008 to 2010, he was a Commissioning Engineer for NARI Technology Company, Ltd., Nanjing, China. From 2013 to 2017, he was an Electrical Engineer for State Grid Corporation of China, Jiangsu, Nanjing, China. His research interests include load modeling, load forecasting, distribution system estimation, machine learning, and power system relaying.